frontiers | Frontiers in Chemical Engineering

TYPE Review
PUBLISHED 05 April 2023
DOI 10.3389/fceng.2023.1144237

OPEN ACCESS

EDITED BY
Congrui Grace Jin,
University of Nebraska-Lincoln,
United States

REVIEWED BY
Runming Tao,
Oak Ridge National Laboratory (DOE),
United States
Lu Yu,
Oak Ridge National Laboratory (DOE),
United States

*CORRESPONDENCE
Ji Wu,
jwu@georgiasouthern.edu
Shaowen Xu,
shaowenxu@georgiasouthern.edu

SPECIALTY SECTION
This article was submitted to Materials Process Engineering, a section of the journal *Frontiers in Chemical Engineering*

RECEIVED 14 January 2023
ACCEPTED 01 February 2023
PUBLISHED 05 April 2023

CITATION
Wu J and Xu S (2023), Manufacturing flow batteries using advanced 3D printing technology—A review.
Front. Chem. Eng. 5:1144237.
doi: 10.3389/fceng.2023.1144237

Manufacturing flow batteries using advanced 3D printing technology—A review

Ji Wu[1]* and Shaowen Xu[2]*

[1]Department of Chemistry and Biochemistry, Georgia Southern University, Statesboro, GA, United States, [2]Department of Mechanical Engineering, Georgia Southern University, Statesboro, GA, United States

In the past decade, electrochemical energy storage systems such as rechargeable batteries have been explored as potential candidates for the large-scale storage of intermittent power sources. Among these, redox flow batteries stand out due to their low fabrication costs, high scalability, and long cycle life. Several redox flow battery pilot plants with MWh capacity have been constructed worldwide, although their commercial profitability is currently under investigation. 3D printing as a burgeoning technology offers unlimited opportunities in the process of optimizing the design, performance, and fabrication cost of redox flow batteries as compared to traditional top-down manufacturing techniques. This review discusses the principles of various redox flow batteries and 3D printing techniques, followed by explaining the advantages, disadvantages, and major factors to consider when using 3D printing in the construction of efficient redox flow batteries. The practical applications of 3D printing for redox flow batteries with different redox chemistries in the past decade are critically summarized, including classical all-vanadium, Zn/Br, and novel competitors. Lastly, a summary is provided along with outlooks that may provide valuable guidance for scientists interested in this research frontier.

KEYWORDS

3D printing, redox flow battery, all vanadium, zinc-bromine, zinc-air, 3-D electrode, enhanced electrochemical performance

1 Introduction

1.1 Significance, principles, and a brief history of redox flow batteries

Non-renewable sources currently dominate the global energy market. The 2018 data from the United States Department of Energy showed that >80% of the energy consumption in the United States was from natural gas, petroleum oil, and coal. The progression of global warming, climate change, and environmental pollution underscores the urgency for the increased utilization of green energies such as solar, wind, and tidal energies. However, these renewable sources are intermittent, thereby requiring the development of efficient energy storage systems to balance the power output. Electrochemical energy storage (EES) systems like batteries are the most promising candidates for the large-scale storage of intermittent energy, among which redox flow batteries (RFBs) stand out due to their low fabrication costs (~$25/kWh on a theoretical base), high scalability (up to MWs), and long cycle life (>10,000 cycles) (Li and Lu, 2020). Lockheed Martin is currently building a 6.5MW/52 MWh GridStar Flow battery energy storage system (BESS) to store solar energy in Canada (https://www.energy-storage.news/

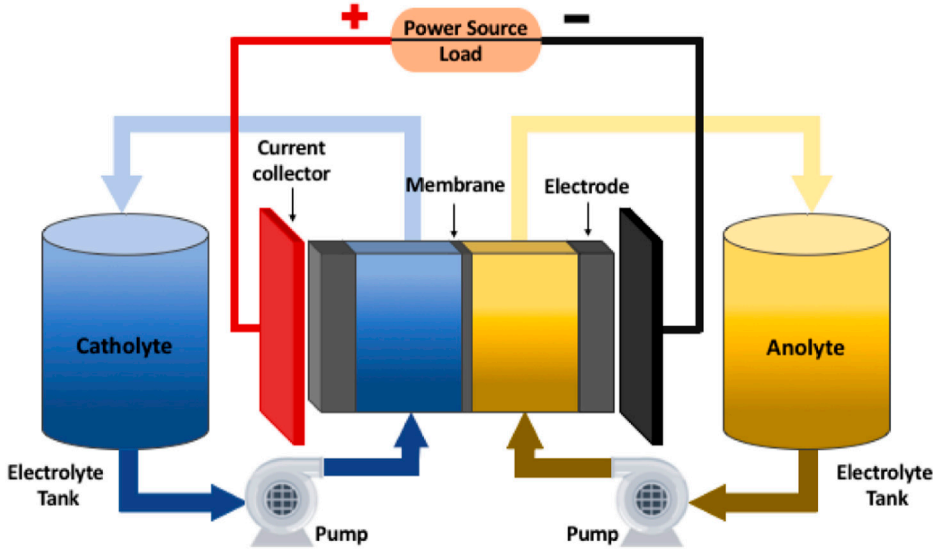

FIGURE 1
General schematic illustration of a redox flow battery. Reproduced under CC-BY-4.0 from Clemente et al. (2020).

first-megawatt-scale-pilot-for-lockheed-martins-flow-battery-at-solar-project-in-canada/) (Subburaj et al., 2015).

Typical RFBs consist of an anolyte, a catholyte, a membrane separator, external storage tanks, pumps, and an AC/DC inverter (Figure 1). The principles of RFB are like those of classical batteries such as lead-acid and lithium-ion batteries, all of which rely on reversible redox reactions to store and release electricity (Arenas et al., 2017). Anolytes are reduced, and catholytes are oxidized during the battery charging process. The stored energy can then be released through the oxidation of anolytes and reduction of catholytes when an external load is applied. However, most redox-active chemical species in RFBs are present only in solutions and stored in external tanks. They are pumped through porous electrodes where redox reactions occur. Additionally, the membrane separator must be ion-selective to prohibit the crossover of redox-active species; otherwise, the stored energy may be self-discharged. In contrast, the redox-active species in commercial lithium-ion batteries are intercalated into the solid electrodes, e.g., graphite and lithium cobalt oxide. Thus, ion-selective membranes are not required (Kim et al., 2019).

The equilibrium cell potential of RFBs at room temperature can be calculated using the simplified Nernst equation shown as follows:

$$E_c = E^{\varnothing} + \frac{0.05916}{n} log \frac{C_{anolyte}}{C_{catholyte}},$$

where E_c is the cell potential at non-standard conditions, E^{ϕ} is the cell potential at standard conditions, and n represents the number of moles of electrons transferred during the redox reaction. Practically, factors other than the one calculated using the Nernst equation can lower the cell potential, including various overpotentials and IR drops. The IR drop originates from the resistances of the anolyte, catholyte, membrane separator, and contacts at the cathode and anode. Major overpotentials occur due to 1) the concentration of polarization at the anode and cathode; and 2) the activation energy needed for cathodic and anodic reactions. Concentration polarization can be partially relieved by promoting turbulent flow and optimizing flow rates to achieve the most efficient mass transport at the electrode surface. The activation energy can be significantly reduced by using effective catalysts and surface chemistry. Lowering the IR drop and overpotentials of RFBs can increase voltage and energy outputs since the specific energy of RFBs is equal to the product of the capacity and cell potential. The capacity of RFBs is directly proportional to the volume of the redox-active electrolytes and the number of electrons transferred. When charge transfer resistance is the rate-limiting step in the electrode kinetics, the well-known Butler–Volmer equation governs the maximum electrical current density in RFBs. When the mass transport of ions is the rate-limiting factor, the following equation applies to the limiting current density:

$$I_{max} = K \times V^{x},$$

where V is the linear velocity of the electrolyte and K is an empirical constant. Notably, the exponent x is greatly affected by the flow type, e.g., 0.3 for laminar flow and >0.5 for turbulent flow (Arenas et al., 2017). In other words, effective turbulent flow benefits a higher current density, as limited by the mass transport of ions (Nelissen et al., 2003; Abbasi-Chianeh and Shokrani, 2021).

The initial concept of RFBs dates back to the 1970s (Gong et al., 2015). Although magnitudes of redox chemistries have been proposed for RFBs since then, only a few warrant extensive investigation for practical applications, including all-vanadium, Zn–Br_2, Zn–air, Fe–Cr, and Zn–ferricyanide RFBs. (Weber et al., 2011) The research on all-vanadium RFBs is most extensive since the use of vanadium ions for both anolytes and catholytes can circumvent the membrane crossover issue of redox-active ions

and, thus, significantly reduce the costs of RFB operation and maintenance (Ponce de León et al., 2006). Many pilot plants of all-vanadium RFBs have been reported in the literature (Walsh and Ponce de León, 2018; Pärnamäe et al., 2020). Unfortunately, vanadium is not abundant in the Earth's crust (~100 ppm), implying that this technology may not be economically sustainable for large-scale applications (Minke and Turek, 2018). Most recently, RFBs made of abundant elements, including Zn-Br_2, Zn-air, Zn-polyiodide, and non-aqueous quinone-based organic RFBs, have been extensively studied (Perry and Weber, 2016; Zhang et al., 2018)

1.2 Important factors to consider for the optimal design of redox flow batteries

As mentioned previously, liquid electrolytes must flow through conductive electrodes to be reduced or oxidized by the electricity from the inverter. Thus, porous electrodes with large surface areas are desirable to enhance the redox reaction efficiency and thereby reduce the energy consumption required to repeatedly pump electrolytes (Arenas et al., 2015). If the pores are too small (sub-mm), the fluidic flow resistance increases exponentially since the thickness of the stagnant liquid layer is comparable to the pore diameter, which may prohibit the mass transport of reactant and product ions and stop redox reactions (Chen et al., 2008; De Wolf et al., 2022). Therefore, the right balance must be reached among the fluidic flow rate, electrochemical reaction rate, and electrode pore size to obtain an optimal design for redox flow batteries. To realize this goal, experimental trials of different parameters must be combined with theoretical fluidic dynamic computations (Messaggi et al., 2018).

1.3 Basics of 3D printing technology

3D printing (a major form of additive manufacturing) is a revolutionary manufacturing process that is the opposite of conventional subtractive processes. Instead of removing material from a solid block of material, 3D printing creates a product from a digital file of a pre-designed computer-aided design (CAD) model using a layer-by-layer additive process. Each of these layers is a thinly sliced cross section of the designed model. This manufacturing process offers the opportunity for not only rapid prototyping of new product designs but also the fabrication of parts with complex geometry not easily made using traditional manufacturing methods.

A wide range of materials is available for 3D printing, including polymer (polylactide (PLA), acrylonitrile butadiene styrene (ABS), polycarbonates (PC), polypropylene (PP), polyethylene terephthalate glycol (PETG), thermoplastic polyurethane (TPU), polyethylenimine (PEI), polyether ether ketone (PEEK), nylon, metal powder (aluminum, copper, bronze, iron, tungsten, steel, and titanium) filaments, polymer resins, ceramic powder (e.g., clay, silicon carbide, zirconium silicate, and borosilicate) filaments, metal (nickel, steel, cobalt, cobalt chrome, titanium, aluminum, copper, and tungsten) powder, ceramic powder, and composites (e.g., carbon fiber HT PLA and carbon-filled nylon).

Numerous 3D printing processes with different principles have been developed, including material extrusion, binder jetting, powder bed fusion, material jetting, VAT photopolymerization (stereolithography 3D printing), directed energy deposition, and sheet lamination. Each of the processes can only be applied to specific materials. For example, material extrusion is mainly used for thermoplastic filaments, metal or ceramic powder/thermoplastic mixed filaments, and fiber/thermoplastic mixed filaments. Powder bed fusion is utilized for metal and polymer powder. Binder jetting is applied to ceramic, metal, and polymer powder, while VAT photopolymerization and material jetting are used to print UV-polymerizable resins. The cost and quality of 3D printing machines depend on the printing process and printing materials. Material extrusion is the most used printing process. The cost of the printer and filament is the lowest ($200–$1,500[20]), but the surface finish (120 μm–280 μm layer thickness) (3ERP, 2023) and accuracy (±200 μm to ± 500 μm) (FORMLABS, 2023) of the printed parts are not impressive. With a slightly higher cost ($500–110,000) (HUBS, 2023), material jetting and VAT photopolymerization offer better accuracy (± 10 μm to ± 100 μm) (FORMLABS, 2023) and a good finish (10 μm–100 μm layer thickness) (3ERP, 2023). In contrast, powder bed fusion, directed energy deposition, and binder jetting machines (80 μm–120 μm layer thickness, accuracy ±100 μm to ±300 μm) (3ERP, 2023) are quite expensive, with purchase prices ranging from $20,000 to $650,000 (FORMLABS, 2023).

The most common material extrusion process is fused deposition modeling (FDM), also known as fused filament fabrication (FFF). FDM creates an object from a digital file of a CAD model by selectively depositing melted filament over a built platform through an extrusion nozzle layer by layer in a predetermined path until it is completed. The object can also be built with two different materials using two extrusion nozzles. The filaments are commonly made of pure thermoplastic polymers. Metal/ceramic parts can be fabricated using metal (ceramic) powder/polymer mixed filaments, followed by de-binding and sintering post-processes. A wide range of materials is available for FDM, including PLA, ABS, PETG, TPU, PEI, PEEK, steel, bronze, copper, aluminum, titanium, and silicon carbide. Direct-ink-writing (DIW) is another material extrusion-based 3D printing method. Instead of using filament, liquid-phase ink is dispensed from a very small nozzle and selectively deposited, layer by layer. This method is usually used for printing fine structures in meso/micro-scales.

Material jetting builds a part in a layer-by-layer manner by selectively depositing and dispensing droplets of liquid resin with ink print-heads; these droplets are simultaneously solidified by UV light exposure. Similarly, VAT photopolymerization creates a part by selectively curing liquid photopolymer resin in a transparent holding tank, followed by washing and UV curing post-processes. The thickness of each layer of these two processes can be controlled down to 10 microns. Therefore, the process offers high accuracy, fine details, and smooth surfaces. Powder bed fusion includes direct metal laser sintering (DMLS), electron beam melting (EBM), selective laser melting (SLM), and selective laser sintering (SLS). In powder bed fusion, a thin layer of powder is spread on the build platform, and a laser or electron beam is then used to selectively melt

and fuse the powder in a layer on the platform. Another layer of powder is then spread over the previous layer, and new layers of the part are built by the laser or electron beam on the previous layers until the part fabrication is complete. The powder materials available for PBF include stainless steel, aluminum, titanium, copper, cobalt chrome, and nylon. Binder jetting creates a part by selectively depositing a liquid-binding agent with a print head onto a thin layer of powder such as ceramic, metal, sand, or composites. A new layer of powder is then spread over the previous layer, and a liquid-binding agent is selectively deposited on the new layer. The process is repeated until the entire part is complete. Once the part is formed, the plastics must be cured. Like FDM, de-binding and sintering processes are required to create a strong solid 3D part for metal or ceramic powder. Directed energy deposition is a more complex material extrusion process typically used with metal in the form of wire or powder. The process deposits materials melted by a laser or electron beam onto a specified surface with a nozzle mounted on a multi-axis arm. This process is generally utilized to repair or add additional material to an existing structural part.

1.4 3D printing for efficient flow batteries: Advantages, disadvantages, and major factors to consider

Due to the nature of the processes, 3D printing offers unlimited opportunities to design and fabricate complex structured parts that cannot be made using traditional manufacturing processes. 3D printing can complete fabrication within hours, speed up prototyping, and allow more efficient design modification. 3D printing also allows the introduction of lightweight porous structures in a solid portion of a product to reduce the mass and cost while increasing the surface area. Taking advantage of the additive process, 3D printing only uses materials needed for the part itself, with no or little wastage, saving energy and materials compared to traditional subtractive processes. Starting from creating the CAD model, 3D printing also allows integration with multi-physics modeling and simulation for structural optimization before printing to improve the performance and reduce the cost of the designed product.

However, the size of the 3D printed part may be limited by the size of the printing platform or chamber. Moreover, the surface finish of the 3D-printed part is often not satisfactory compared to that of a part fabricated by traditional manufacturing processes; thus, post-processing is needed to achieve the required finish. Due to the layer-by-layer printing process, the printed part is not homogenous and the layer-to-layer interface is relatively weak compared to bulk materials. Thus, the part could delaminate under certain loading conditions along the interface. This issue can be improved for metal parts by heat treatment. Another potential issue is the accuracy of the 3D-printed part. Due to the lower tolerances of some printers or part shrinkage after post-processing, the final dimensions may differ from those of the original design. Hence, all potential factors for dimension change should be considered when the initial design is created. Finally, 3D printing technology cannot currently be applied to all materials, although a wide range of materials is available.

In the past decade, 3D printing technology has attracted increasing attention and has been utilized for the design and performance improvement of flow batteries,e.g., studying the structural effects of flow frames (Zhang et al., 2018) and 3D-structured electrodes (Zhang et al., 2018) on battery performance. Due to the strong acid or base working environments of 3D-printed parts, the 3D printing material must be carefully selected according to the chemical activity of various electrolytes. For example, ABS cannot be used for a part under strong acid concentration conditions or for long-term use. Table 1 summarizes different 3D printing techniques for various RFBs reported by different researchers.

2 3D printing for vanadium redox flow batteries

2.1 Basics of vanadium RFBs

The anolyte and catholyte in classical vanadium RFBs are divided by a porous membrane separator that allows the transport of non-redox-active ions but hinders the mixing of redox-active vanadium ions between the two-half cells. Ion-selective membranes like Nafion are highly favorable, but the high cost is problematic for practical applications (Jiang et al., 2016; Tempelman et al., 2020). Most recently, microporous inorganic/organic membranes have been explored to replace the expensive Nafion membrane (Tempelman et al., 2020). Thus far, their electrochemical performance is comparatively inferior. Carbon-based porous electrodes are routinely used in vanadium RFB because of their high surface area, low cost, chemical inertness, and outstanding electrical conductivity (Kaneko et al., 1991). The porous electrodes can be fabricated by 3D printing or graphite felts/papers. Various spinning methods have been employed to make polyacrylonitrile (PAN) fibers that are then pyrolyzed at high temperatures to obtain graphite felts (Langner et al., 2016). However, the poor mechanical strength of porous carbon materials may lower the charging and discharging efficiency after long-term operation. The redox reactions of vanadium RFBs are shown as follows (Kear et al., 2012):

$$VO_2^+ + 2H^+ + e^- \rightleftharpoons VO^{2+} + H_2O \quad (1)$$

$$V^{2+} \rightleftharpoons V^{3+} + e^- \quad (2)$$

During the discharging process, reaction (1) occurs at the anode and reaction (2) happens at the cathode. The two reactions are reversed when charging the RFB. The higher the anolyte and catholyte concentrations, the larger the RFB capacity. When the concentration of electrolytes is too high, the viscous fluids may not be able to flow through the porous electrodes, and vanadium electrolytes may precipitate to block the membrane pores. Lastly, strong acids/bases are widely used in vanadium RFBs as needed to balance the charges and enhance the solubility of vanadium ions. The high corrosiveness may reduce the lifespan of the containers, electrodes, and packing materials, which demands thoughtful consideration during battery design.

2.2 Practical applications of 3D printing for vanadium RFB

Sun et al. built a miniature VRFB prototype with a 3D-printed flow frame and complex internal flow channels (Rajarathnam et al., 2016; Sun et al., 2018; Sun et al., 2019; Adelusi et al., 2020). The

TABLE 1 Applications of 3D printing technology for the development of redox flow batteries.

Name of the part	3D printing method	Material	Type of RFB	Author
Flow frames	FDM 3D printer	Acrylonitrile butadiene styrene	Zn–Ce flow battery	Arenas et al. (2017)
Frame structures of the cell	FDM 3D printer	Cellulose-based biodegradable polypropylene filament	Zn–air battery	Nagy et al. (2022)
Frame of the half-flow cell	UV-cured 3D printer	UV-cured acrylic	Zn–Ce redox-flow batteries	Periyapperuma et al. (2017)
Multi-channel electrodes	Laser sintering 3D printer	Stainless steel	Rechargeable liquid-state Zn–air batteries	Men et al. (2022)
Foam electrodes	N/A	Titanium	$ZnBr_2$ single cell	Pang et al. (2020)
Customized tools (retractable pistons)	Stereolithography 3D printer	UV-polymerizable resins	$ZnBr_2$ battery	Biswas et al. (2017)
Mold for 3D structured electrodes	FDM printer	Polystyrene	Iron–zinc redox flow battery	De Wolf et al. (2022)
Composite electrode	Direct-ink-writing 3D printer	Go/Super-P	Vanadium redox flow battery	Li et al. (2022)
3D-printed structured flow through electrodes	Direct-ink-writing 3D printer	Go/water	Redox flow battery	Beck et al. (2021)
Flow cell	FDM printer	Polyvinylidene fluoride	Vanadium redox flow battery	Schilling et al. (2022)
Static mixers and electrodes	Material jetting polymer 3D printer	UV-polymerizable resins	Vanadium redox flow battery cell	Percin et al. (2018)
Flow frame with complex internal flow channels	Stereolithography 3D printer	UV-polymerizable resins	Vanadium redox flow battery	Sun et al. (2019)
Flow cell manifold	FDM printer	Polypropylene and acrylonitrile butadiene styrene	Vanadium redox flow battery	O'Connor et al. (2022)
Microfluidic networks	Material jetting polymer 3D printer	UV-polymerizable resins	N/A	Marschewski et al. (2017)

frame (Figure 2) was designed, and a numerical model was built using SolidWorks 3D modeling software and then fabricated with a professional-grade high-resolution stereolithography (SLA) 3D printer (Objet30 Pro). The designed frame was modified, fabricated, and tested multiple times to achieve the best results. The results of the study demonstrated that the 3D printed flow configuration in the frame increased the diffusion limit of the vanadium redox chemical species and resulted in much higher performance compared to the H-cell. The energy efficiency finally achieved 40%–45.2% with 0.4 M vanadium redox species. A Coulombic efficiency (η_C), voltage efficiency (η_V), and energy efficiency (η_E) of 58.7, 77.1, and 45.1, respectively, were obtained using the flow cell design and 0.4 M commercial V_2O_5. The Coulombic efficiency remained stable for up to 20 cycles. Percin et al. introduced 3D-printed static mixers and electrodes in a vanadium redox flow battery cell (Figure 3) (Percin et al., 2018). The static mixers were designed as a single layer of twisted filaments with a helical structure (adapted from Fritzmann et al.), fabricated on a Stratasys Objet Eden 260 V material jetting polymer printer and coated with a conductive graphite layer. The static mixers increased the interaction of its surface with particles (activated carbons or graphite powder) in the slurry and increased the contact area of the current collector with the particles in the slurry, thus permitting a better charge transfer between the electrode and particles, as well as the current collector surface and particles. The results revealed that the static mixers reduced the mass transport limitations and increased the cutoff current density, leading to 95% CE and 65% EE in cyclic charge–discharge experiments. Additionally, no large cell overpotential was observed below 20 mA cm^{-2} but it became apparent above 120 mA cm^{-2}. The authors did not prepare cells using traditional methods for comparison.

Li, Q. et al. proposed a porous reduced graphene oxide (r-GO)/Super-P aerogel composite electrode for vanadium redox flow batteries (Figure 4) (Li et al., 2022). First, the GO latticework was printed by a direct ink writing method (DIW) with a GO/Super-P device. The latticework was then freeze-dried, reduced in HI solution, water rinsed, and finally dried to form porous aerogel composite electrodes. Several composite electrodes with different compositions and mass ratios were fabricated and studied. The results demonstrated a discharge capacity of a VRFB cell with the optimized rGO-P electrode of 848.4 mA h at a current density of 80 mA cm^{-2}, which was 14.9% higher than that of the traditional GF electrode due to the hierarchical porous structure, high specific surface area, and relatively high conductivity of the rGO-P electrode.

Similarly, Beck et al. proposed 3D-printed structured flow-through electrodes for flow batteries (Figure 5) (Beck et al., 2021). Both SC and FCC lattice-based structures were fabricated and studied. The electrode structure was printed using the direct ink writing method and a water-based GO solution. The structure was then frozen in liquid nitrogen and freeze-dried to form an aerogel. Finally, the aerogel was carbonized to produce a porous structured flow-through electrode. The authors characterized the structures of the flow-through electrodes and performed CFD simulation and mass transfer analysis. The engineered flow in the electrodes

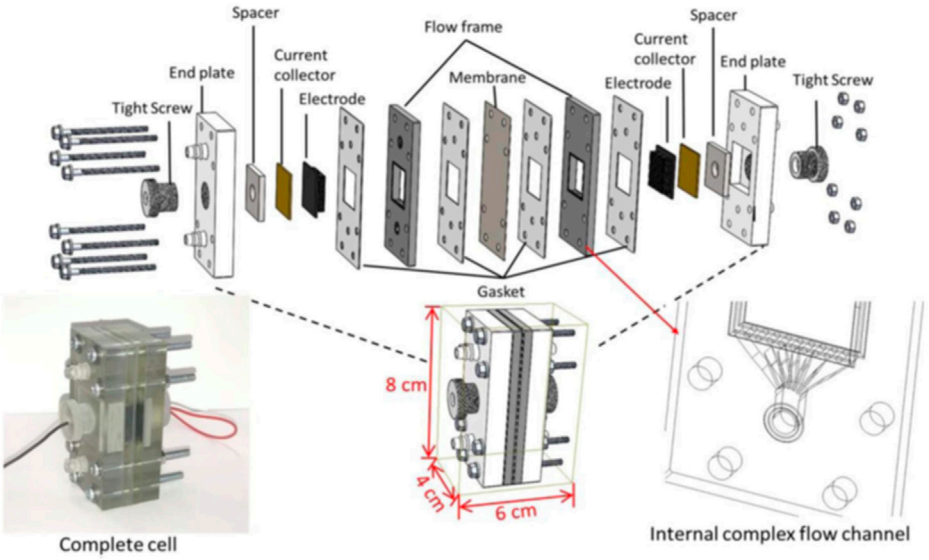

FIGURE 2
Structure and assembly miniature of a VRFB prototype, Reproduced under CC-BY-4.0 from Sun et al. (2019).

FIGURE 3
The geometry of the static mixers. Based on data from Percin et al. (2018).

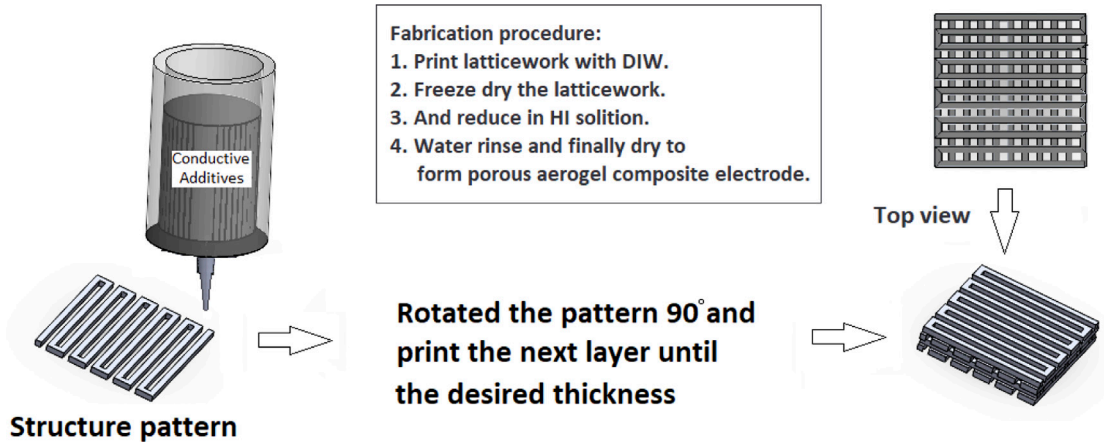

FIGURE 4
Diagram of the printing process. Based on data from Li et al. (2022).

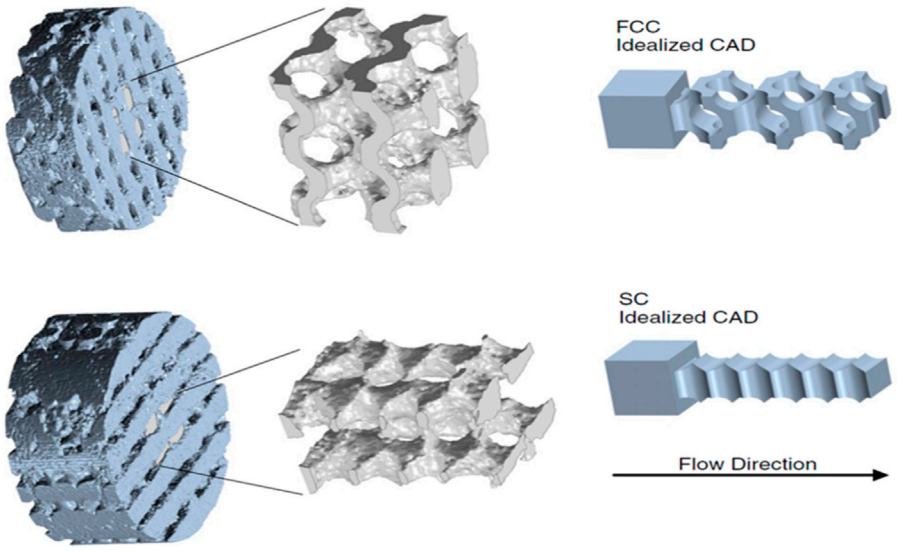

FIGURE 5
Tomographic reconstruction of representative 3D-printed FCC (top) and SC (bottom) electrodes and idealized CAD representation of the void region with an entrance region added to allow for simulation. Reproduced from Beck et al. (2021), with permission from PNAS.

produced by the 3D-printed structures induced a stagnation zone, increased the surface strain rate, and dramatically enhanced mass transfer in the thin boundary layer of the flow near the wall of the electrodes. The authors also reported that a better printing resolution could continually improve the performance of 3D flow-through electrodes. An excellent mass transfer rate of $>10^2$ s^{-1} was achieved using $Fe(CN)^{-3}/^{-4}$ redox couples, which was claimed to be the highest reported value in the literature. However, they did not assess Coulombic efficiency, cell overpotential, and cycling performance. Both studies discussed previously demonstrated the usefulness of 3D printing technology for rapid prototyping to refine and develop new components for highly efficient flow batteries.

Schilling et al. (2022) utilized 3D printing to build a flow cell to gain insights into the reactions and transport processes and determine the optimized operating conditions to improve VRFB efficiency. The authors investigated the influence of carbon material, flow rate, vanadium and sulfuric acid concentrations, operating temperature, vanadium species and electrochemical reaction, applied potential, and charge stage. The developed characterization technique provided valuable data for selecting electrode materials and determining optimal operating conditions.

O'Connor et al. (2022) performed a comprehensive study of 3D-printed VRFB test cells. They designed cells using SolidWorks CAD software. Electrochemical-CFD coupled simulations were integrated into the design and optimization of the manifold of flow cells. The effect of printing parameters on the quality of the 3D-printed manifolds was studied. The optimized manifold design was fabricated on an Ultimaker S5 FDM 3D printer using PP or ABS

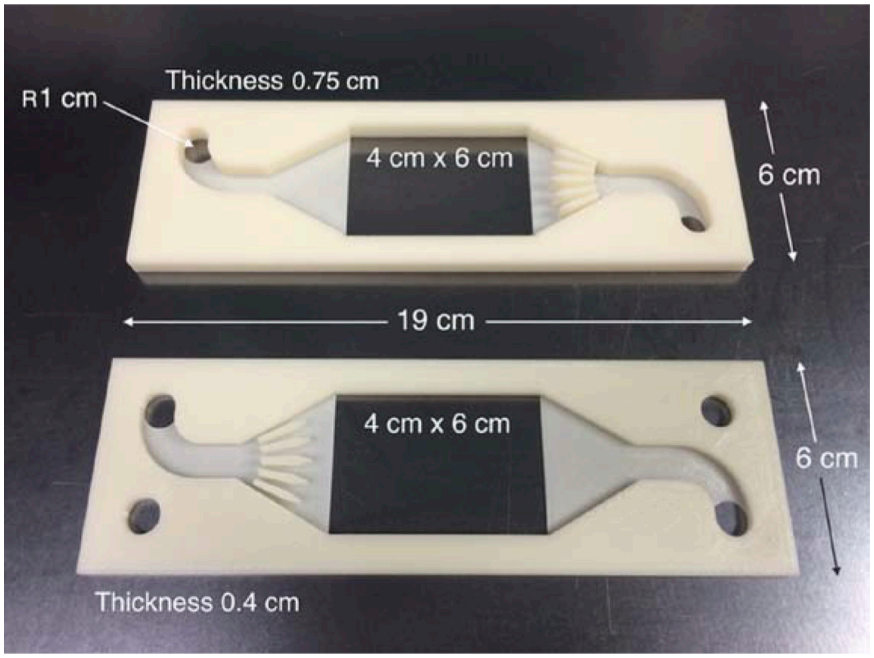

FIGURE 6
3D printed flow frames for uniform electrolyte flows in Zn-Ce Flow Battery. Reproduced under CC-BY-4.0 from Arenas et al. (2015; ref. 16).

filaments with printing parameters optimized for chemical compatibility and charge–discharge tests. The chemical compatibility tests were carried out for polypropylene (PP) and acrylonitrile butadiene styrene (ABS) 3D-printed flow cells using several commonly used aqueous and non-aqueous solvents and electrolytes. Finally, the cost of the 3D-printed cell was also approximated. Fifteen cells were cycled at 50 mA cm^{-2} between 1.10 V and 1.75 V, with an average CE close to 80%. The results suggested that ABS was chemically compatible with many commonly used aqueous flow battery electrolytes and a well-suited polymer for the fabrication of 3D-printed flow cells. Moreover, the optimized printing parameters provided a good starting point for the fabrication of high-quality cells, 3D printing was an extremely cost-effective method for the fabrication of customized flow cells and the development of new cell structures, and integrating electrochemical-CFD-coupled simulations into the design was an efficient pathway and could provide critical feedback for the refinement of flow cell structures.

3 3D printing for zinc–bromine redox flow batteries

Since the concept of Zn–Br RFB was initially proposed in 1977, the technology has steadily advanced to near-maturity for commercialization in the past five decades (Rajarathnam et al., 2016). The Zn–Br RFB anode is made of solid Zn metal, while the cathode Br_2 is in a liquid state at room temperature. Therefore, Zn–Br is also called a hybrid RFB as it differs from the classical liquid–liquid vanadium RFB. During the discharging process, the solid Zn metal is stripped and liquid Br_2 is reduced to Br^-, as shown as follows (Adelusi et al., 2020):

$$Br_2 + 2e^- \rightleftharpoons 2Br^- \quad (3)$$

$$Zn \rightleftharpoons Zn^{2+} + 2e^- \quad (4)$$

The overall calculated cell potential at standard conditions, 1.85 V, is higher than ~1.2 V for vanadium RFBs. The aforementioned reactions are reversed during the charging process. Like vanadium RFBs, Nafion separators have been widely used in Zn-RFBs due to their high ion selectivity and Coulombic efficiency. Dialysis membranes and dialysis membranes coated with Nafion have also been developed to lower the membrane cost. However, the formation of Zn dendrites after repeated stripping/plating must be addressed due to potential safety concerns (Xu et al., 2020). Compared to vanadium RFB, Zn–Br RFB has the advantages of low costs, high capacity and energy density, and high stability (Zhang et al., 2019). Br_2 is used instead of Cl_2 due to the large solubility of $ZnBr_2$ and the higher toxicity of chlorine gas. The theoretical specific energy of Zn RFB is an estimated 428 Wh kg^{-1}, higher than that of commercial lithium-ion batteries (Yuan et al., 2019). However, the practical energy density of Zn–Br RFB is only ~50–60 Wh kg^{-1} (Chakrabarti et al., 2014).

Pang et al. (2020) used 3D-printed titanium foam electrodes instead of traditional graphite electrodes in a Zn/Br single cell. Due to their porous structures, the titanium foam electrodes also acted as a current collection column, resulting in an optimal cell structure. The test results demonstrated the high energy efficiency and reliability of the proposed $ZnBr_2$ single cell. The Coulombic efficiency of the test cell was ~72% after 50 cycles at a current density of 30 mA cm^{-2}, corresponding to an energy density of 40.45 Wh kg^{-1}, significantly higher than that of cells fabricated using classical methods. In another study, Biswas et al. (2017) used 3D printing to make customized tools (retractable pistons) to synthesize carbon foam electrodes for a zinc-bromine battery. The cells operated stably with >90% Coulombic and >60% energy efficiencies for >1,000 cycles, with an energy density of 9 W h L^{-1}.

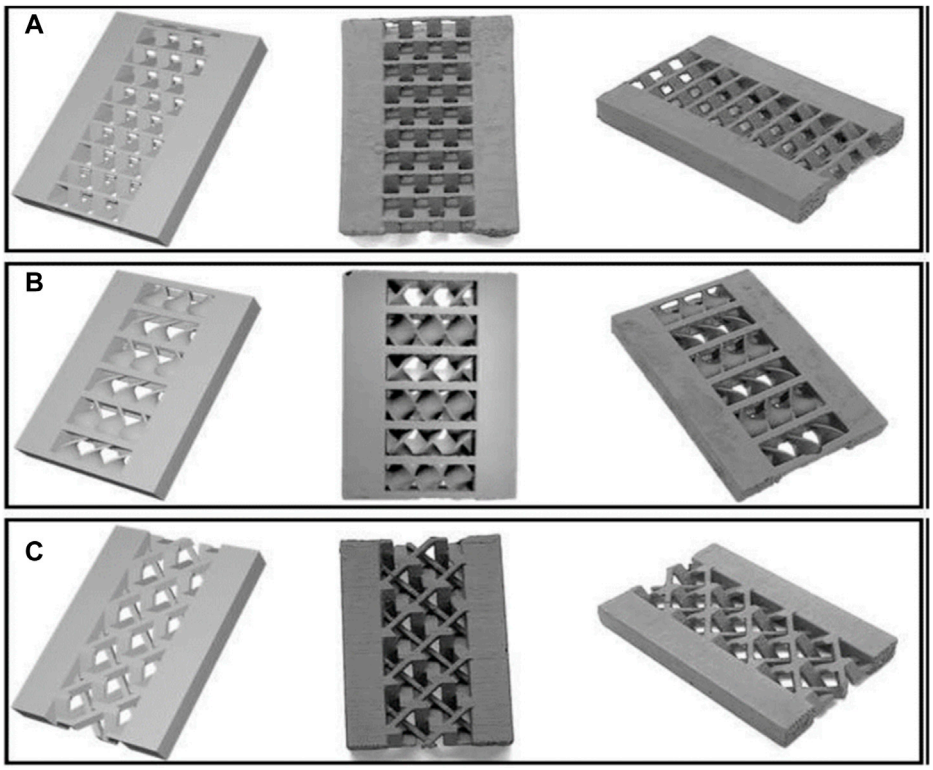

FIGURE 7
Structures of 3D electrodes: **(A)** RLPD, **(B)** Kenics, and **(C)** SMX electrodes. Reproduced from De Wolf et al. (2022), with permission from ChemElectroChem, Wiley Online Library.

4 3D printing for burgeoning redox flow batteries

Novel RFBs have been intensively investigated in the past decade, aiming to further reduce fabrication costs and operation/maintenance expenditures and overcome the shortcomings of classical RFBs (Zhang et al., 2018). Zn–Ce and V–Ce RFBs are particularly notable due to their high cell voltages and potential for commercialization (Yun et al., 2015; Xie et al., 2022). Organic and polymeric redox species have also attracted research attention, although they are still in laboratory development (Wei et al., 2017; Winsberg et al., 2017). Several articles deserve special attention regarding 3D printing technology for the improvement of Zn–Ce and V–Ce RFBs, as discussed in the following paragraphs.

Arenas et al. (2016) applied 3D printing technology to fabricate negative and positive electrode flow frames for Zn–Ce flow battery cells with ABS filaments to introduce uniform electrolyte flow (Figure 6). The parts were fabricated using an Up Plus two FDM printer with ABS filaments. This high-precision (200 μm resolution) 3D printer offered accurate dimensions and a small tolerance for the fabricated parts. Although ABS is less chemically resistant, it can be used under low acid conditions and 20–50°C temperature conditions for a relatively short testing period without major issues. The flow channels were characterized by the pressure drops at the inlet and outlet of each half of the cell and compared to the FM01-LC reactor. The results revealed an asymmetry between the two half-cells; i.e., the pressure drop on the positive side was similar to that observed in the FM01-LC cell, whereas a large pressure drop was observed on the negative side at the same flow velocity, indicating that modification of the flow frames was required to reduce the pressure drop. In other words, different flow channel patterns should be designed for various electrolytes, and computational fluid dynamic (CFD) simulation should be involved in flow channel design. The authors designed and printed two types of 3D-printed polymer turbulence promoters and reported the need for more design refinement, fine structures, and a new printing method with fine resolution to obtain the profiled turbulence promoters to improve the mass transport rate. No other electrochemical tests were reported in this work, which focused solely on the flow dynamics of 3D-printed half cells.

To reduce the high-pressure drop and operating costs, De Wolf et al. (2022) introduced 3D-structured electrodes into a redox flow battery. Several derivate structures of the Kenics, Ross low-pressure drop (RLPD), and Sulzer (SMX) mixers were fabricated and studied (Figure 7). The authors also investigated the influence of the geometry of different 3D-structured electrodes on the performance. The electrodes were made using an indirect 3D printing method. Ti/epoxy/glycerol paste was cast in a 3D mold, which was printed by an Ultimaker 3 FDM printer using polystyrene. After the paste was cured by heating, the mold was dissolved by toluene to produce Ti/epoxy/glycerol composite structures. The organic materials in the green part were then removed and the part was sintered to form 3D Ti electrodes. Finally, graphite layers were coated on the surface of the brown parts to achieve sufficient electrochemical activity. Compared to

laser sintering 3D printing, the cost of the proposed method was much lower. Alternative methods to fabricate Ti composite structures are available using FDM printers with Ti powder filament. The research results demonstrated that 1) the structured electrode minimized dead zones in the flow paths; 2) more uniform flow distributions could be obtained; 3) the flow battery with structured electrodes could be operated at higher current densities; and 4) the proposed 3D-structured electrodes showed similar electrode potentials compared to conventional disordered carbon felt electrodes, even at two or three orders of magnitude lower pumping power. Of note, this work = investigated cell hydrodynamics at a current density of 0–120 mA cm^{-2} but did not assess cycling, polarization, and Coulombic efficiency.

Men et al., 2022 developed 3D-printed multi-channel electrodes inspired by xylem structures of wood, aiming to improve the active surface area and enhance mass transfer in cathodes of zinc-air batteries due to enhanced oxygen reduction reaction efficiency and power output. The multi-channel structures promoted a continuous supply of oxygen from the air and formed a massive tri-phase boundary in the cathode. The bio-inspired multi-channel electrodes were made of stainless steel on an EOSINT M280 laser sintering 3D printer. The authors studied the effects of channel size on the mass transfer efficiency and determined the optimal channel size (600 μm). The zinc-air batteries with bio-inspired multi-channel cathodes were characterized by excellent electrochemical performance including high power density and an open-circuit voltage. The optimized structures offered high-efficiency mass transfer channels and relatively large surface areas for catalysts, resulting in power densities up to 170 mW cm^{-2}.

Marschewski et al. introduced 3D-printed microfluidic networks in miniaturized flow cells (alkaline-based redox) to efficiently deliver power and manage heating and cooling of the electronic components (Marschewski et al., 2017). The microfluidic network frames were printed using a high-resolution material jetting printer (ProJet HD 3000Plus) with plastic (VisiJet EX200 Plastic). Then, 1 μm nickel and 0.4 carbon layers were sequentially sputter-coated on the frames. In total, four kinds of microfluidic network structures were fabricated and the effects of the structures on the cell performance were studied. The results demonstrated that the RFC with tapered multiple-pass microfluidic networks gained up to 1.4 W cm^{-2} power densities with 0.99 W cm^{-2} net power densities at room temperature. Thus, rational tailoring of fluidic networks is crucial for the development of devices to effectively combine power delivery and thermal management. The results demonstrated the potential for the direct integration of RFB with electronic components to simultaneously generate power and cool electronic components.

3D printing technology also features high design flexibility and fast prototyping for the development of flow batteries. Periyapperuma et al. (2017)fabricated a flow half-cell prototype using a UV-cured 3D printer for the development of Zn-Ce redox-flow batteries. The authors used an acrylic that was chemically stable for the selected ionic liquid electrolyte to print the cell, investigate the impact of concentration and flow rate on the Zn^{2+}/Zn^{0} electrochemical performance and Zn morphology, and determine an optimized Zn^{2+} concentration and flow rate. A cycling efficiency of 45% was achieved at a higher electrolyte concentration (18 mol%) compared to a 33% efficiency for an electrolyte concentration of 9 mol%. The results also provided suggestions for upgrading the flow cell configuration to improve the cycling performance of redox flow batteries. Nagy et al. (2022) also used3D printing to fabricate an environmentally friendly high-performance prototype of a rechargeable Zn-air battery. The frame structures of the battery were printed using a Prusa i3 MK3S 3D FDM printer and cellulose-based biodegradable polypropylene (PP) filament. Both horizontal and vertical cell setups were printed and studied. The effect of the molecular weight of CMC–Na on battery performance and Zn electrode reaction cyclic voltammetry was investigated. No zinc dendrite and mossy formation were observed in over 1,000 cycles, with an impressive 100% coulomb efficiency. Another study used 3D printing to make customized tools to synthesize carbon foam electrodes in a zinc-bromine battery (Biswas et al., 2017).

5 Summary and outlook

3D printing, as a new, advanced manufacturing technology and the opposite of traditional material removal processes, can be applied to easily build complex structured components that could not be fabricated using traditional manufacturing methods. This technology can be used to build parts with structures having two or more length scales. 3D printing allows for complete design, modification, and fabrication within hours, thereby significantly speeding prototyping in engineering development. The technology has attracted increasing attention and has been applied to flow battery parts/cell design, part modification, and performance improvement. Research in the past decade has demonstrated that 3D printing is a low-cost and efficient manufacturing method for the rapid prototyping of parts or flow cells and a useful and efficient method to manufacture parts to study the structural effects of electrolyte flow frame and 3D-structured electrodes on the mass transfer and performance of flow batteries. When integrated with multi-physics modeling and simulation, 3D printing technology is a powerful tool for structural optimization and performance improvement in advanced flow batteries.

DFM printers are the most common and economical method used for the fabrication of 3D-printed parts. However, surface finishing is generally not high, and post-processing is needed when high surface finishing is required. In contrast, stereolithography 3D printers offer very good surface finishing. Both powder bed fusion 3D-printed Ti parts and Ti-coated DFM-printed parts have been used as electrodes for improving the efficiency of mass transfer. 3D-printed metal parts are strong but expensive, while metal-coated DFM-printed parts are economical to produce but have much less strength. Due to the strong acid or base working environments in flow batteries, the 3D printing materials should be carefully selected based on the chemical activity of the electrolytes. Although the chemical compatibilities of polypropylene and acrylonitrile butadiene styrene have been studied for strong acid/base environments, more materials need to be explored, such as polyvinyl chloride, polytetrafluoroethylene, polyether ether ketone, and high-density polyethylene. Heating and cooling systems should be integrated into the architectural design of the flow batteries since temperature may affect battery efficiency. Moreover, advanced dynamic fluidic computations for different redox flow batteries must be developed to provide more meaningful data and guidance for the design of RFB parts fabricated using various 3D printers. Lastly, machine learning/artificial intelligence is another promising approach for structure optimization and cell development. Given the abundance of RFB research data, machine learning/artificial

intelligence may provide useful guidance regarding material selection, electrode structure optimization, and cell design.

Author contributions

JW and SX contributed equally to this review from the concept outline to the manuscript preparation. Both authors contributed to the article and approved the submitted version.

Acknowledgments

JW and SX acknowledge the generous support provided by Georgia Southern University.

Conflict of interest

The authors declare that the research was conducted in the absence of any commercial or financial relationships that could be construed as a potential conflict of interest.

Publisher's note

All claims expressed in this article are solely those of the authors and do not necessarily represent those of their affiliated organizations, or those of the publisher, the editors, and the reviewers. Any product that may be evaluated in this article, or claim that may be made by its manufacturer, is not guaranteed or endorsed by the publisher.

References

3ERP, 2023 3ERP (2023). 3ERP. Available at: https://www.3erp.com/blog/how-dimensionally-accurate-are-3d-printed-parts/#:~:text=The%20accuracy%20of%20a%20desktop,is%20around%20%C2%B1%200.2%20mm (Accessed 01 27, 2023).

Abbasi-Chianeh, V., and Shokrani, F. (2021). Turbulent fluid flow-assisted rapid electrodeposition of Zn–Ni γ-phase from modified Watt's type bath by addition of saccharin. *Bull. Mater. Sci.* 44 (3), 238. doi:10.1007/s12034-021-02509-z

Adelusi, I., Victor, A. C., Andrieux, F., and Dawson, R. (2020). Practical development of a ZnBr2 flow battery with a fluidized bed anode zinc-electrode. *J. Electrochem. Soc.* 167 (5), 050504. doi:10.1149/2.0112005jes

Arenas, L. F., León, C. P. d., and Walsh, F. C. (2016). Mass transport and active area of porous Pt/Ti electrodes for the Zn-Ce redox flow battery determined from limiting current measurements. *Electrochimica Acta* 221, 154–166. doi:10.1016/j.electacta.2016.10.097

Arenas, L. F., Ponce de León, C., and Walsh, F. C. (2017). Engineering aspects of the design, construction and performance of modular redox flow batteries for energy storage. *J. Energy Storage* 11, 119–153. doi:10.1016/j.est.2017.02.007

Arenas, L. F., Walsh, F. C., and de León, C. P. (2015). 3D-Printing of redox flow batteries for energy storage: A rapid prototype laboratory cell. *ECS J. Solid State Sci. Technol.* 4 (4), P3080–P3085. doi:10.1149/2.0141504jss

Beck, V. A., Ivanovskaya, A. N., Chandrasekaran, S., Forien, J.-B., Baker, S. E., Duoss, E. B., et al. (2021). Inertially enhanced mass transport using 3D-printed porous flow-through electrodes with periodic lattice structures. *Proc. Natl. Acad. Sci.* 118 (32), e2025562118. doi:10.1073/pnas.2025562118

Biswas, S., Senju, A., Mohr, R., Hodson, T., Karthikeyan, N., Knehr, K. W., et al. (2017). Minimal architecture zinc–bromine battery for low cost electrochemical energy storage. *Energy and Environ. Sci.* 10 (1), 114–120. doi:10.1039/c6ee02782b

Chakrabarti, M. H., Mjalli, F. S., AlNashef, I. M., Hashim, M. A., Hussain, M. A., Bahadori, L., et al. (2014). Prospects of applying ionic liquids and deep eutectic solvents for renewable energy storage by means of redox flow batteries. *Renew. Sustain. Energy Rev.* 30, 254–270. doi:10.1016/j.rser.2013.10.004

Chen, F., Mourhatch, R., Tsotsis, T. T., and Sahimi, M. (2008). Pore network model of transport and separation of binary gas mixtures in nanoporous membranes. *J. Membr. Sci.* 315 (1), 48–57. doi:10.1016/j.memsci.2008.02.005

Clemente, A., Ramos, G. A., and Costa-Castelló, R. (2020). Voltage H∞ control of a vanadium redox flow battery. *Electronics* 9 (10), 1567. doi:10.3390/electronics9101567

De Wolf, R., De Rop, M., and Hereijgers, J. (2022). Effects of structured 3D electrodes on the performance of redox flow batteries. *ChemElectroChem* 9 (22), e202200640. doi:10.1002/celc.202201028

FORMLABS (2023). Formlabs. Available at: https://formlabs.com/blog/how-to-calculate-3d-printer-cost (Accessed 01 26, 2023).

Gong, K., Fang, Q., Gu, S., Li, S. F. Y., and Yan, Y. (2015). Nonaqueous redox-flow batteries: Organic solvents, supporting electrolytes, and redox pairs. *Energy and Environ. Sci.* 8 (12), 3515–3530. doi:10.1039/c5ee02341f

HUBS (2023). HUBS. Available at: https://www.hubs.com/knowledge-base/impact-layer-height-3d-print/(Accessed 01 27, 2023).

Jiang, B., Wu, L., Yu, L., Qiu, X., and Xi, J. (2016). A comparative study of Nafion series membranes for vanadium redox flow batteries. *J. Membr. Sci.* 510, 18–26. doi:10.1016/j.memsci.2016.03.007

Kaneko, H., Nozaki, K., Wada, Y., Aoki, T., Negishi, A., and Kamimoto, M. (1991). Vanadium redox reactions and carbon electrodes for vanadium redox flow battery. *Electrochimica Acta* 36 (7), 1191–1196. doi:10.1016/0013-4686(91)85108-j

Kear, G., Shah, A. A., and Walsh, F. C. (2012). Development of the all-vanadium redox flow battery for energy storage: A review of technological, financial and policy aspects. *Int. J. Energy Res.* 36 (11), 1105–1120. doi:10.1002/er.1863

Kim, T., Song, W., Son, D.-Y., Ono, L. K., and Qi, Y. (2019). Lithium-ion batteries: Outlook on present, future, and hybridized technologies. *J. Mater. Chem. A* 7 (7), 2942–2964. doi:10.1039/c8ta10513h

Langner, J., Bruns, M., Dixon, D., Nefedov, A., Wöll, C., Scheiba, F., et al. (2016). Surface properties and graphitization of polyacrylonitrile based fiber electrodes affecting the negative half-cell reaction in vanadium redox flow batteries. *J. Power Sources* 321, 210–218. doi:10.1016/j.jpowsour.2016.04.128

Li, Q., Dong, Q., Wang, J., Xue, Z., Li, J., Yu, M., et al. (2022). Direct ink writing (DIW) of graphene aerogel composite electrode for vanadium redox flow battery. *J. Power Sources* 542, 231810. doi:10.1016/j.jpowsour.2022.231810

Li, Z., and Lu, Y.-C. (2020). Material design of aqueous redox flow batteries: Fundamental challenges and mitigation strategies. *Adv. Mater.* 32 (47), 2002132. doi:10.1002/adma.202002132

Marschewski, J., Brenner, L., Ebejer, N., Ruch, P., Michel, B., and Poulikakos, D. (2017). 3D-printed fluidic networks for high-power-density heat-managing miniaturized redox flow batteries. *Energy and Environ. Sci.* 10 (3), 780–787. doi:10.1039/c6ee03192g

Men, X., Li, Z., Yang, W., Wang, M., Liang, S., Sun, H., et al. (2022). 3D-Printed bio-inspired multi-channel cathodes for zinc–air battery applications. *J. Bionic Eng.* 19 (4), 1014–1023. doi:10.1007/s42235-022-00173-5

Messaggi, M., Canzi, P., Mereu, R., Baricci, A., Inzoli, F., Casalegno, A., et al. (2018). Analysis of flow field design on vanadium redox flow battery performance: Development of 3D computational fluid dynamic model and experimental validation. *Appl. Energy* 228, 1057–1070. doi:10.1016/j.apenergy.2018.06.148

Minke, C., and Turek, T. (2018). Materials, system designs and modelling approaches in techno-economic assessment of all-vanadium redox flow batteries – a review. *J. Power Sources* 376, 66–81. doi:10.1016/j.jpowsour.2017.11.058

Nagy, T., Nagy, L., Erdélyi, Z., Baradács, E., Deák, G., Zsuga, M., et al. (2022). Environmentally friendly high performance Zn-air rechargeable battery using cellulose derivatives: A 3D-printed prototype. *J. Energy Storage* 49, 104173. doi:10.1016/j.est.2022.104173

Nelissen, G., Van Den Bossche, B., Deconinck, J., Van Theemsche, A., and Dan, C. (2003). Laminar and turbulent mass transfer simulations in a parallel plate reactor. *J. Appl. Electrochem.* 33 (10), 863–873. doi:10.1023/a:1025811727594

O'Connor, H., Bailey, J. J., Istrate, O. M., Klusener, P. A. A., Watson, R., Glover, S., et al. (2022). An open-source platform for 3D-printed redox flow battery test cells. *Sustain. Energy and Fuels* 6 (6), 1529–1540. doi:10.1039/d1se01851e

Pang, Z., Gong, Y., Yuan, M., and Li, X. (2020). A newly designed modular ZnBr2 single cell structure. *Batteries* 6 (2), 27. doi:10.3390/batteries6020027

Pärnamäe, R., Gurreri, L., Post, J., van Egmond, W. J., Culcasi, A., Saakes, M., et al. (2020). The acid–base flow battery: Sustainable energy storage via reversible water dissociation with bipolar membranes. *Membranes* 10 (12), 409. doi:10.3390/membranes10120409

Percin, K., Rommerskirchen, A., Sengpiel, R., Gendel, Y., and Wessling, M. (2018). 3D-printed conductive static mixers enable all-vanadium redox flow battery using slurry electrodes. *J. Power Sources* 379, 228–233. doi:10.1016/j.jpowsour.2018.01.061

Periyapperuma, K., Zhang, Y., MacFarlane, D. R., Forsyth, M., Pozo-Gonzalo, C., and Howlett, P. C. (2017). Towards higher energy density redox-flow batteries: Imidazolium ionic liquid for Zn electrochemistry in flow environment. *ChemElectroChem* 4 (5), 1051–1058. doi:10.1002/celc.201600875

Perry, M. L., and Weber, A. Z. (2016). Advanced redox-flow batteries: A perspective. *J. Electrochem. Soc.* 163 (1), A5064–A5067. doi:10.1149/2.0101601jes

Ponce de León, C., Frías-Ferrer, A., González-García, J., Szánto, D. A., and Walsh, F. C. (2006). Redox flow cells for energy conversion. *J. Power Sources* 160 (1), 716–732. doi:10.1016/j.jpowsour.2006.02.095

Rajarathnam, G. P., and Vassallo, A. M. (2016). "Description of the Zn/Br RFB system," in *The zinc/bromine flow battery: Materials challenges and practical solutions for technology advancement*. Editors G. P. Rajarathnam and A. M. Vassallo (Singapore: Springer Singapore), 11–28.

Schilling, M., Braig, M., Köble, K., and Zeis, R. (2022). Investigating the V(IV)/V(V) electrode reaction in a vanadium redox flow battery – a distribution of relaxation times analysis. *Electrochimica Acta* 430, 141058. doi:10.1016/j.electacta.2022.141058

Subburaj, A. S., Pushpakaran, B. N., and Bayne, S. B. (2015). Overview of grid connected renewable energy based battery projects in USA. *Renew. Sustain. Energy Rev.* 45, 219–234. doi:10.1016/j.rser.2015.01.052

Sun, H., Takahashi, H., Kamada, Y., Sato, K., Matsushima, Y., Khosla, A., et al. (2018). Vanadium redox flow batteries fabricated by 3D printing and employing recycled vanadium collected from ammonia slag. *ECS Trans.* 88 (1), 269–278. doi:10.1149/08801.0269ecst

Sun, H., Takahashi, H., Nishiumi, N., Kamada, Y., Sato, K., Nedu, K., et al. (2019). Vanadium redox flow batteries fabricated by 3D printing and employing recycled vanadium collected from ammonia slag. *J. Electrochem. Soc.* 166 (9), B3125–B3130. doi:10.1149/2.0251909jes

Tempelman, C. H. L., Jacobs, J. F., Balzer, R. M., and Degirmenci, V. (2020). Membranes for all vanadium redox flow batteries. *J. Energy Storage* 32, 101754. doi:10.1016/j.est.2020.101754

Walsh, F. C., and Ponce de León, C. (2018). Progress in electrochemical flow reactors for laboratory and pilot scale processing. *Electrochimica Acta* 280, 121–148. doi:10.1016/j.electacta.2018.05.027

Weber, A. Z., Mench, M. M., Meyers, J. P., Ross, P. N., Gostick, J. T., and Liu, Q. (2011). Redox flow batteries: A review. *J. Appl. Electrochem.* 41 (10), 1137–1164. doi:10.1007/s10800-011-0348-2

Wei, X., Pan, W., Duan, W., Hollas, A., Yang, Z., Li, B., et al. (2017). Materials and systems for organic redox flow batteries: Status and challenges. *ACS Energy Lett.* 2 (9), 2187–2204. doi:10.1021/acsenergylett.7b00650

Winsberg, J., Hagemann, T., Janoschka, T., Hager, M. D., and Schubert, U. S. (2017). Redox-flow batteries: From metals to organic redox-active materials. *Angew. Chem. Int. Ed.* 56 (3), 686–711. doi:10.1002/anie.201604925

Xie, X., Mushtaq, F., Wang, Q., and Daoud, W. A. (2022). The renaissance of the Zn-Ce flow battery: Dual-membrane configuration enables unprecedentedly high efficiency. *ACS Energy Lett.* 7 (10), 3484–3491. doi:10.1021/acsenergylett.2c01646

Xu, Z., Fan, Q., Li, Y., Wang, J., and Lund, P. D. (2020). Review of zinc dendrite formation in zinc bromine redox flow battery. *Renew. Sustain. Energy Rev.* 127, 109838. doi:10.1016/j.rser.2020.109838

Yuan, Z., Yin, Y., Xie, C., Zhang, H., Yao, Y., and Li, X. (2019). Advanced materials for zinc-based flow battery: Development and challenge. *Adv. Mater.* 31 (50), 1902025. doi:10.1002/adma.201902025

Yun, S., Parrondo, J., and Ramani, V. (2015). A vanadium–cerium redox flow battery with an anion-exchange membrane separator. *ChemPlusChem* 80 (2), 412–421. doi:10.1002/cplu.201402096

Zhang, C., Zhang, L., Ding, Y., Peng, S., Guo, X., Zhao, Y., et al. (2018). Progress and prospects of next-generation redox flow batteries. *Energy Storage Mater.* 15, 324–350. doi:10.1016/j.ensm.2018.06.008

Zhang, H., Lu, W., and Li, X. (2019). Progress and perspectives of flow battery technologies. *Electrochem. Energy Rev.* 2 (3), 492–506. doi:10.1007/s41918-019-00047-1